UC San Diego
UC San Diego Previously Published Works

Title

Fast quantitative 3D ultrashort echo time MRI of cortical bone using extended cones sampling

Permalink

https://escholarship.org/uc/item/9mq6q7zp

Journal

Magnetic Resonance in Medicine, 82(1)

ISSN

0740-3194

Authors

Wan, Lidi
Zhao, Wei
Ma, Yajun
et al.

Publication Date

2019-07-01

DOI

10.1002/mrm.27715

Peer reviewed

FULL PAPER

Fast quantitative 3D ultrashort echo time MRI of cortical bone using extended cones sampling

Lidi Wan[1,2] (ID) | **Wei Zhao[1]** | **Yajun Ma[1]** | **Saeed Jerban[1]** | **Adam C. Searleman[1]** | **Michael Carl[4]** | **Eric Y. Chang[1,3]** | **Guangyu Tang[2]** | **Jiang Du[1]**

[1]Department of Radiology, University of California, San Diego, California

[2]Department of Radiology, Shanghai Tenth People's Hospital of Tongji University, School of Medicine, Shanghai, China

[3]Radiology Service, VA San Diego Healthcare System, San Diego, California

[4]GE Healthcare, San Diego, California

Correspondence
Jiang Du, Department of Radiology, University of California, 9500 Gilman Drive, San Diego, CA 92093.
Email: jiangdu@ucsd.edu

Purpose: To investigate the effect of stretching sampling window on quantitative 3D ultrashort TE (UTE) imaging of cortical bone at 3 T.

Methods: Ten bovine cortical bone and 17 human tibial midshaft samples were imaged with a 3T clinical MRI scanner using an 8-channel knee coil. Quantitative 3D UTE imaging biomarkers, including T_1, T_2^*, magnetization transfer ratio and magnetization transfer modeling, were performed using radial or spiral Cones sampling trajectories with various durations. Errors in UTE-MRI biomarkers as a function of sampling time were evaluated using radial sampling as a reference standard.

Results: For both bovine and human cortical bone samples, no significant differences were observed for all UTE biomarkers (single-component T_2^*, bicomponent T_2^* and relative fractions, T_1, magnetization transfer ratio, and magnetization transfer modeling of macromolecular fraction) for spiral sampling windows of 992 μs to 1600 μs compared with a radial sampling window of 688 μs.

Conclusion: The total scan time can be reduced by 76% with quantification errors less than 5%. Quantitative UTE-MRI techniques can be greatly accelerated using longer sampling windows without significant quantification errors.

KEYWORDS
cortical bone, quantitative, sampling window, UTE imaging

1 | INTRODUCTION

Cortical bone accounts for approximately 80% of the skeleton mass.[1] Cortical bone microstructure plays a critical role in determining the risk of fracture and is altered by diseases such as osteoporosis, hyperparathyroidism, renal disease and diabetes, which often have diffuse effects on bone metabolism and remodeling.[2-5] With the rapidly growing prevalence of osteoporosis, fragility fractures have become a major public health concern, motivating the urgent need to develop noninvasive clinical biomarkers of cortical bone strength, elasticity, and toughness.[6,7]

Cortical bone consists of approximately 40% mineral, 35% collagen, and 25% water by volume.[8] Previous NMR spectroscopy studies have demonstrated that the cortical bone MR signal has multiple components that differ by T_2 values.[9] The short T_2 signals (T_2 values vary from 12-400 μs) originate from collagen backbone and side-chain protons, as

well as from collagen-bound water, whereas longer T_2 signals (T_2 values on the order of milliseconds or longer) are primarily from pore water and lipid methylene protons. The short T_2 components predominately result in a mean T_2 value of approximately 0.42-0.50 ms[10]; therefore, conventional MRI sequences with TEs of several milliseconds or longer detect little or no signal from cortical bone.

Ultrashort echo time (UTE) MRI sequences with TEs on the order of microseconds allow for direct imaging and quantitative assessment of cortical bone.[1] A series of techniques including dual-echo UTE acquisition with echo subtraction, long T_2 saturation UTE imaging, UTE with off-resonance saturation, as well as single and dual adiabatic inversion-recovery UTE techniques have been developed for high-contrast imaging of cortical bone.[11-14] Notably, the short T_2 component detected by UTE is predominantly from bound water: Collagen backbone protons give no signal on UTE sequences,[15] but can be measured indirectly by magnetization transfer (MT) methods.[16]

A series of quantitative UTE MRI techniques have been developed to evaluate cortical bone.[1] These biomarkers include T_1,[17] single-component apparent T_2^*,[18] bicomponent analysis of bound and pore water T_2^* and relative fractions,[19] magnetization transfer ratio (MTR),[20] and MT modeling of water and macromolecular fractions with their exchange rates.[21] These biomarkers have been shown to be related to key biomechanical properties of cortical bone. For instance, bound water was found to be positively associated with bone strength and toughness, whereas free water was inversely related to modulus of elasticity.[22,23] Magnetization transfer ratio has shown significant correlations with bone porosity and bone mechanics.[24] Recently, MT modeling was found to be capable of detecting ex vivo bone stress injuries.[25] However, UTE biomarkers have not been used widely in the clinical setting, with 1 major limitation being the long scan time.

For short T_2 species, the signals may decay significantly during the process of RF excitation and data acquisition.[10,26] To minimize TE, UTE sequences begin data acquisition at the center of k-space and use non-Cartesian sampling. The decay of the signal along the sampling trajectory to outer k-space can result in blurring of short T_2 components. Radial sampling (PR) is often used in UTE sequences to minimize short T_2 blurring, but has a long scan time because fully sampling outer k-space is inefficient.[27] The total scan time can be reduced by using more efficient sampling patterns, such as those using twisted radial or spiral trajectories.[28,29] Both Rahmer et al[26] and Du et al[27] found that the reduction of scan time using these trajectories is limited by short T_2 blurring, as the sampling window is lengthened. A number of UTE biomarkers including T_1, T_2^*, MTR, and MT modeling of water and macromolecular proton fractions have been developed for quantitative assessment of cortical bone.[1,14] To the best of our knowledge, the effect of extending the sampling window on those quantitative UTE biomarkers has not been investigated systematically.

The purpose of this study was to quantitatively analyze the errors associated with extending the sampling duration on 3D quantitative UTE-MRI of midshaft tibia cortical bone (which represents a low spatial resolution short T_2 object). These results were used to develop an optimized protocol for quantitative imaging of cortical bone that represents a balance between speed and quantification errors, thus facilitating the clinical use of quantitative UTE-MRI.

2 | METHODS

2.1 | Sample preparation

Cortical bone specimens were harvested from 10 fresh bovine samples and 17 fresh-frozen human tibial midshafts from 15 donors (67 ± 24 years old, 7 females and 8 males). The human bone specimens were provided by a nonprofit whole-body donation company (United Tissue Network, Phoenix, AZ), whereas the bovine bone samples were obtained from a local slaughter house. All bone specimens were cut to 3 cm in length using a Delta ShopMaster band saw (Delta Machinery). The bone marrow and other soft tissues were removed with a scalpel to get higher SNR, as tissue noise from surrounding muscle and marrow fat is greatly reduced). The bone specimens were equilibrated for at least 2 hours in phosphate-buffered saline to minimize trapped gas, then put in a plastic container filled with Fomblin, to minimize dehydration and susceptibility before scanning. All scans were performed at room temperature.

2.2 | Ultrashort TE–MR imaging

All imaging was performed on a 3T clinical MRI scanner (MR750, GE Healthcare Technologies, Milwaukee, WI) using an 8-channel knee coil. The maximum gradient amplitude, slew rate, and ramp time were 50 mT/m, 200 T/m/s and 250 μs, respectively. The maximum gradient amplitude used in this experiment was 45 mT/m for PR and all Cones acquisitions; the maximum slew rate was 182 T/m/s for PR and 128 T/m/s for all Cones acquisitions. All 3D UTE sequences used a short rectangular excitation pulse followed by 3D radial or spiral sampling with various data acquisition window lengths (Figure 1A,B).

Three-dimensional regridding with a Kaiser-Bessel kernel was used for reconstruction. After regridding, a Fermi filter was applied to the k-space data to reduce Gibbs ringing. Then, a fast Fourier transform was applied to the filtered data to generate the multichannel images. Finally, a commonly used sum-of-squares method was used for multichannel image combination.
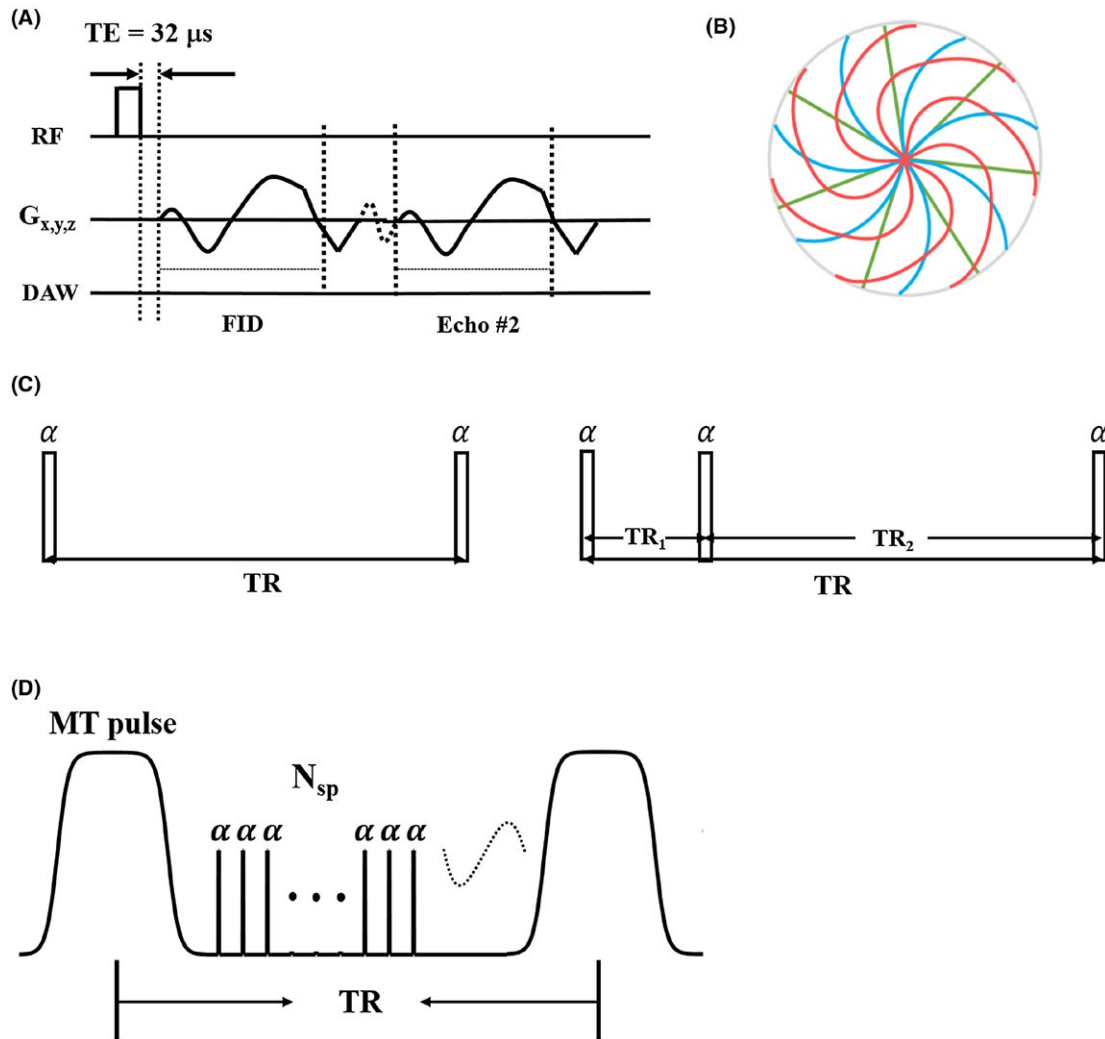
FIGURE 1 Ultrashort TE (UTE) pulse sequence diagram and trajectories. A, For 3D UTE sequences, a short rectangular hard pulse excitation is followed by 3D radial or spiral sampling. Three-dimensional dual-echo UTE was used for acquisition with the first short TE of 32 μs. B, Two-dimensional representation of example trajectories: radial trajectory (green line), spiral trajectory with short sampling window (blue line), and spiral trajectory with longer sampling window (pink line). As the sampling window is increased, the spiral trajectories have greater curvature and more k-space coverage with each spoke. Note that radial sampling has the shortest sampling window length, but that all trajectories oversample central k-space. C, Conventional 3D UTE Cones (3D UTE-Cones) sequence with single-Cones actual flip angle imaging (AFI) sequences uses a pair of interleaved TRs for accurate B_1 mapping, which together with the variable TR (VTR) method provides T_1 measurement. D, A Fermi pulse was used for MT preparation followed by multiple-spoke (Nsp) excitation. Scan time can be reduced by a factor of N_{sp}. Abbreviation: DAW, data acquisition window

Three quantitative imaging protocols were performed: (1) a dual-echo 3D-UTE sequence (TR = 100 ms; 5 dual TE = 0.032/2.2, 0.2/4.4, 0.4/6.6, 0.6/8.8, and 0.8/11 ms; flip angle (FA) = 10°) for single and bicomponent T_2^* analysis (Figure 1A)[30]; (2) a 3D UTE actual FA imaging (AFI) variable TR (VTR) method for accurate T_1 mapping (AFI: TR = 20/100 ms, FA = 45°; VTR: TR = 20, 30, 50, and 100 ms; FA = 45°) (Figure 1C)[31,32]; and (3) a 3D UTE-MT sequence (MT saturation power = 500°, 1000°, and 1500°; frequency offset = 2, 5, 10, 20, and 50 kHz; TR = 100 ms; FA = 10°; 11 spokes per MT preparation to accelerate the scan) (Figure 1D) to measure the MTR in addition to

2-pool MT modeling of water and macromolecular proton fractions and exchange rates. Other imaging parameters included FOV = 6 × 6 × 4 cm³, acquisition matrix = 128 × 128 × 20, and readout bandwidth = 62.5 kHz. The Nyquist requirement was fulfilled for all data acquisitions. The designed k-space (i.e., ellipsoid) was used for the raw data filling with a lower resolution in the slice direction. All k-z data were used for regridding reconstruction. (In ellipsoid sampling, the k-z gradient was scaled down to achieve the prescribed slice thickness. The number of cones was reduced so that only 20 slices were acquired and reconstructed during regridding reconstruction).

To investigate the effect of extended sampling window on quantitative UTE imaging, each of these sequences was repeated using several sampling trajectories: PR and several Cones trajectories (spiral trajectories with conical view ordering) with different stretch factors (Figure 1B). Ramp sampling was used for all acquisitions in both PR and Cones sequences. Gradient delay was measured to correct the radial and spiral trajectories.[33] For both bovine and human bone samples, the PR trajectory had a sampling time of 688 μs. The Cones sampling times were 992 (Cones with a stretching factor of 1.0 μs, or Cones1.0), 1200 μs (Cones1.2), 1392 μs (Cones1.4) and 1600 μs (Cones1.6), corresponding to acceleration factors of 2.6, 3.5, 4.1 and 5.0 over PR sampling, respectively. The stretching factor was defined as the ratio of sampling window using the stretched spiral sampling over sampling window using the PR trajectory, whereas the acceleration factor was defined as the ratio of total scan time of PR sequence to each Cones sequence. For example, the scan times for dual-echo 3D-UTE imaging with radial trajectory and these spiral trajectories were 9.75, 3.67, 2.80, 2.32 and 1.95 minutes, respectively. There are 5327, 4813, 3639, 2943, and 2473 projections for PR and Cones with a stretch factor of 1, 1.2, 1.4 and 1.6, respectively.

2.3 | Data analysis

The analysis algorithm was written in MATLAB (MathWorks, Natick, MA) using the Levenberg-Marquardt method for nonlinear least-squares curve fitting and was executed offline on DICOM images obtained by the protocols described previously. Regions of interest (ROIs) were manually drawn on the first UTE image of each series, then copied to each of the subsequent images. The mean intensities within each of the ROIs were used for curve fitting. Single-component ($S(TE) \propto \exp(-TE/T2^*) + constant$) and bicomponent ($S(TE) \propto F_S \times \exp(-TE/T2_S^*) + F_L \times \exp(-TE/T2_L^*) + constant$) fitting models were used for T_2^* decay analyses acquired from the dual-echo 3D-UTE-Cones sequence. Bicomponent analysis estimates the T_2^* and relative fractions of a short T_2^* component and a long T_2^* component, presumably the bound and pore water pools, respectively.[30] The value of T_1 was analyzed from the 3D UTE-AFI and UTE-VTR sequences using single-component fitting.[29] The UTE-MT data set was analyzed for MTR[34] and with a 2-pool model[21] to estimate the macromolecular fraction. The ROIs were carefully drawn on the outer two-thirds band of cortical bone to avoid signal contamination from residual bone marrow fat near the endosteal surface.

2.4 | Statistical analysis

After all data analyses, error percentages in UTE-MRI biomarkers from spiral trajectories were determined for each measured parameter using results from radial sampling as a reference standard. Statistical analyses were performed using SPSS software (IBM, Armonk, NY)[24] and the R statistical computing environment (version 3.5.1). One-way analysis of variance with 2-sided Dunnett's test was used for the significance of the mean differences of all biomarkers compared with radial sampling. The null hypothesis of the omnibus
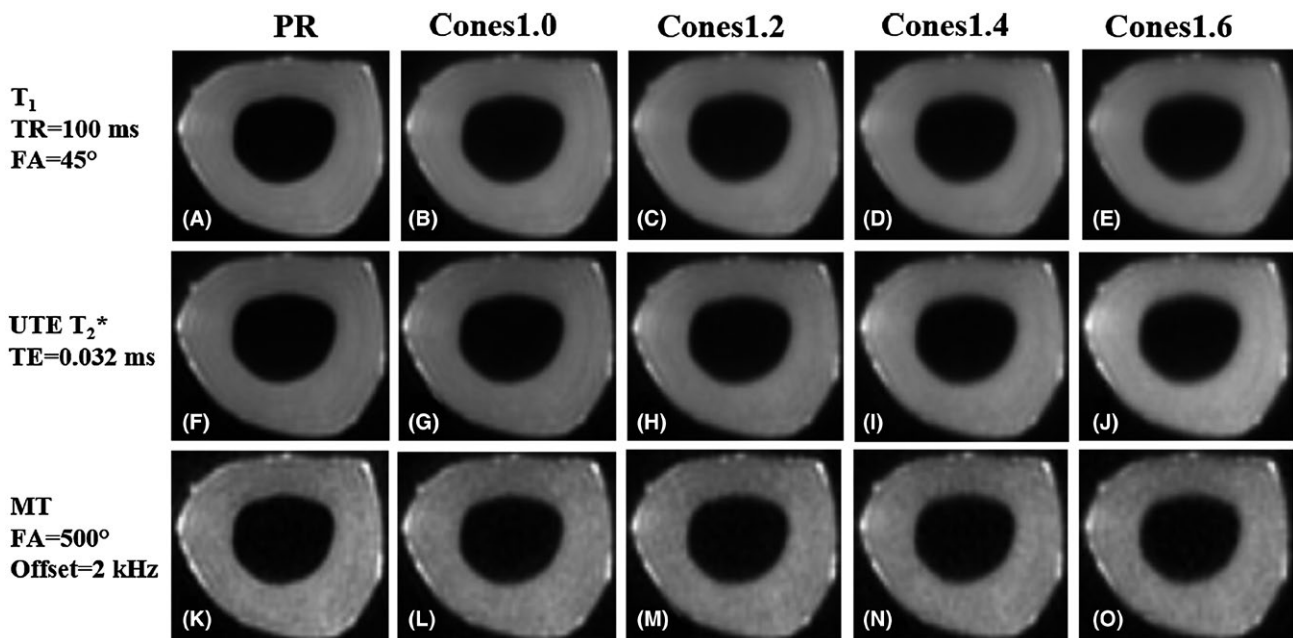

FIGURE 2 Representative T_1 (A-E), T_2 (F-J), and MT (K-O) magnitude images of the same bovine bone sample with different sampling windows: radial (A,F,K), cones1.0 (B,G,L), cones1.2 (Mm), cones1.4 (D,I,N), and cones1.6 (E,J,O)

analysis of variance test was that the mean was the same for all evaluated trajectories. Bland-Altman analysis was used for agreement assessment of the spiral sampling windows compared with radial sampling. P values less than 0.05 were considered statistically significant.

3 | RESULTS

Figure 2 shows UTE images of a representative bovine cortical bone sample with gradually increasing sampling windows from radial (688 μs) to Cones with a stretching factor of 5.0 (1600 μs). Blurring was more visually apparent with increasing stretching factor. Similarly, Figure 3 shows UTE images of a representative human cortical bone sample with gradually increasing sampling windows from radial (688 μs) to Cones1.6 (1600 μs). The images looked more blurred with increasing stretching factor due to short T_2 decay of cortical bone. With longer sampling duration, off-resonance ringing artifacts from residual endosteal fat also became more prominent. The qualitative effects of extended sampling windows were observed to be similar.

Figure 4 shows the signal intensity curves of 2 representative ROIs of bovine and human cortical bone samples with different sampling windows. The signal intensity of T_1, T_2^*, and MT images in both bovine and human bones have a decreasing trend from PR to longer Cones sampling windows, indicating that extending the sampling window leads to signal loss. The most obvious signal intensity losses were observed from PR to Cones 1.0, while

the changes were relatively small among different Cones sampling windows.

Table 1 indicates the mean and SD of all biomarkers of 10 bovine bone samples, along with percent error and P values from 1-way analysis of variance with Dunnett's test using the PR results as the reference standard. There were no significant differences (all P values > 0.05) for any biomarker when the sampling window length was 1600 μs or lower. For T_1, errors were all within 2%, whereas errors of macromolecular fraction were all within 3% when the sampling window was 1600 μs, which has an acceleration factor of 5.0 over radial sampling. Increased errors in MTR were observed with longer sampling windows, with errors less than 2% with an acceleration factor of 5.0. For longer sampling windows, increased errors were also observed in both the single-component and bicomponent T_2^* analyses, including single-component T_2^*, long T_2^*, and short T_2^* fraction, with errors of single-component T_2^*, short T_2^*, and long T_2^* within 3% when the sampling window was 1392 μs and within 5% for all T_2^* biomarkers when the sampling window was 1600 μs. Although errors of T_2^* biomarkers were all less than 5% with an acceleration factor of 5.0, the error ranges were relatively large, especially single-component T_2^*, when compared with T_1, MTR, and macromolecular fraction.

Table 2 lists the mean and SD of all biomarkers of 17 human bone samples, along with percent error and P values from 1-way analysis of variance with Dunnett's test using the PR results as the reference standard. No significant differences (all P values > 0.05) were observed for any biomarker when the sampling window was 1600 μs or lower. As for the
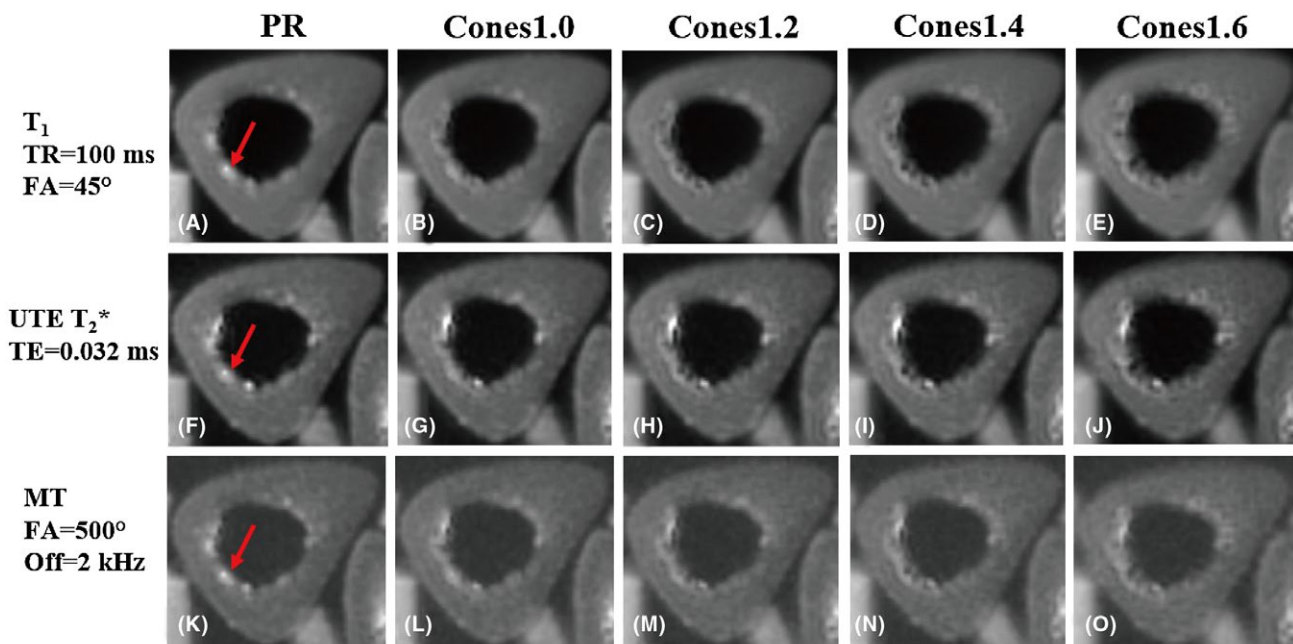

FIGURE 3 Representative T_1 (A-E), T_2 (F-J), and MT (K-O) magnitude images of the same human tibial bone specimen with different sampling windows: radial (A,F,K), cones1.0 (B,G,L), cones1.2 (C,H,M), cones1.4 (D,I,N), and cones1.6 (E,J,O)
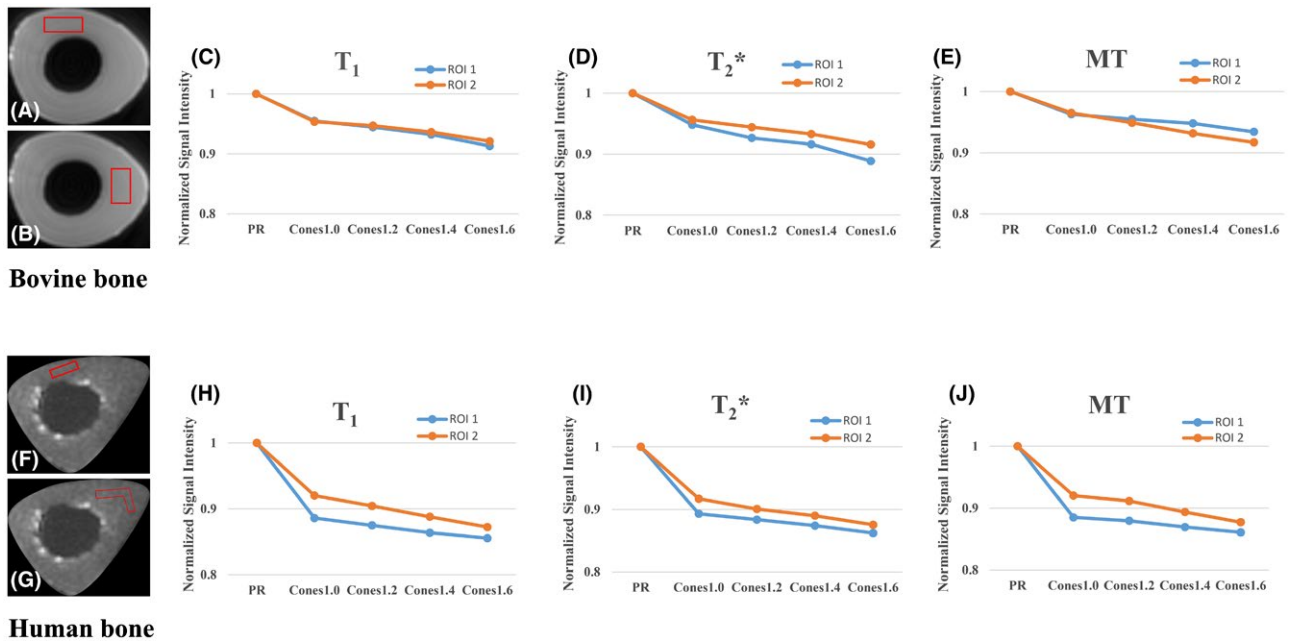
FIGURE 4 Signal intensity variation of T_1 (TR = 200, flip angle [FA] = 45°, TE = 32 μs), T_2^* (TR = 100, FA = 10°, TE = 32 μs), and magnetization transfer (MT) (FA = 500°, offset = 2000, TE = 32 μs) images with different sampling windows (radial sampling [PR]: 688 μs; Cones 1.0: 992 μs, Cones 1.2: 1200 μs, Cones 1.4: 1392 μs, Cones 1.6: 1600 μs) of 2 representative ROIs for bovine (A,B) and human (F,G) bone samples. The corresponding signal intensity variation curves of T_1, T_2^*, and MT were shown in (C), (D) and (E), respectively, for bovine bone, and shown in (H), (I), and (J) for human bone, and were normalized to the PR signal intensities

TABLE 1 Mean and SD of MR properties in bovine bone samples

Mean ± SD (Error %)		PR	Cones1.0	Cones1.2	Cones1.4	Cones1.6
T_2^* single component (ms)		0.45 ± 0.06	0.46 ± 0.06 (1.79%)	0.46 ± 0.06 (2.19%)	0.47 ± 0.06 (2.98%)	0.47 ± 0.05 (4.76%)
	P value		0.99	0.99	0.94	0.80
T_2^* bicomponent	T_{2S}^* (ms)	0.27 ± 0.01	0.27 ± 0.01 (−1.67%)	0.26 ± 0.01 (−2.57%)	0.26 ± 0.01 (−2.55%)	0.26 ± 0.01 (−2.69%)
	P value		0.93	0.42	0.22	0.22
	T_{2L}^* (ms)	2.45 ± 0.68	2.42 ± 0.68 (−1.15%)	2.40 ± 0.67 (−2.07%)	2.38 ± 0.64 (−2.90%)	2.37 ± 0.63 (−3.40%)
	P value		1.00	1.00	1.00	1.00
	Fraction short (%)	75.5 ± 6.3	74.3 ± 6.2 (−1.54%)	73.7 ± 5.9 (−2.37%)	73.1 ± 5.8 (−3.13%)	72.3 ± 5.6 (−4.28%)
	P value		0.98	0.91	0.79	0.57
T_1 (ms)		234.4 ± 10.9	231.9 ± 10.4 (−1.03%)	231.1 ± 10.4 (−1.37%)	232.8 ± 9.9 (−0.68%)	231.9 ± 10.0 (−1.05%)
	P value		0.96	0.89	0.99	0.96
MTR (%) (1500°, 2 kHz)		0.54 ± 0.10	0.54 ± 0.09 (0.67%)	0.54 ± 0.09 (0.74%)	0.54 ± 0.09 (0.89%)	0.55 ± 0.10 (1.66%)
	P value		1.00	1.00	1.00	1.00
Macromolecular fraction (%)		62.3 ± 9.3	63.8 ± 9.3 (2.42%)	64.0 ± 9.4 (2.74%)	62.4 ± 9.3 (0.16%)	63.9 ± 10.0 (2.43%)
	P value		0.99	0.98	1.00	0.99
Sampling window (μs)		688	992	1200	1392	1600
Acceleration factor		1	2.6	3.5	4.1	5.0

Note: Errors (%) and *P* values from Dunnett's test compare the results of each UTE Cones trajectory with PR results.

T_1 macromolecular fraction, the errors were almost within 1% when sampling windows were lower than 1600 μs, other than macromolecular fraction with a 1.13% error when the sampling window was 1200 μs. Errors of single-component T_2^* and long T_2^* were all within 2%, whereas relatively larger errors were observed for short T_2^* and short T_2^* fraction. Increased errors were observed with longer sampling window in short T_2^* and short T_2^* fraction as well as MTR; however, errors were typically less than 5% with an acceleration factor of 4.1.

Figure 5 shows the Bland-Altman plots of all biomarkers (T_1, macromolecular fraction, MTR, T_2^*, short T_2^*, long T_2^*, and short T_2^* fraction) for bovine cortical bone samples. The difference between Cones and radial sampling trajectories and the average of each measurement comprise the axes. The 95% limits of agreement between biomarkers obtained from various Cones trajectories and radial trajectory were −9.88 and 5.05 for T_1, −2.35 and 4.76 for MT modeling of macromolecular fraction, −0.020 and 0.031 for MTR, −0.023 and 0.050 for single-component T_2^*, −0.019 and 0.007 for short T_2^*, −0.36 and 0.24 for long T_2^*, and −6.55 and 2.28 for short T_2^* fraction. There were no significant trends in the distribution of errors as the Cones stretch factor was increased.

Figure 6 shows the Bland-Altman plots of all the biomarkers (T_1, macromolecular fraction, MTR, T_2^*, short T_2^*, long T_2^*, and short T_2^* fraction) for human cortical bone samples. The 95% limits of agreement between biomarkers obtained from various Cones trajectories and radial trajectory were −5.13 and 8.38 for T_1, −5.46 and 4.75 for MT modeling of macromolecular fraction, −0.029 and −0.003 for MTR, −0.048 and 0.058 for single-component T_2^*, −0.051 and 0.028 for short T_2^*, −0.74 and 0.91 for long T_2^*, and −4.91 and 1.19 for short T_2^* fraction. There were no significant differences in the distribution of errors as the Cones stretch factor was increased, although there was a slight trend toward decreased short T_2^* fraction as the stretch factor increased.

4 | DISCUSSION

Quantitative biomarkers derived using 3D Cones UTE-MRI techniques have many potential clinical applications in musculoskeletal system imaging, but the relatively long scan time is a significant barrier for widespread clinical adoption. This study investigated the effects of sampling window on several quantitative 3D Cones UTE-MRI techniques, aiming to

TABLE 2 Mean and SD of MR properties in human bone specimens

Mean ± SD (Error %)		PR	Cones1.0	Cones1.2	Cones1.4	Cones1.6
T_2^* single component (ms)		0.45 ± 0.13	0.46 ± 0.15 (1.47%)	0.46 ± 0.15 (0.82%)	0.46 ± 0.15 (0.95%)	0.46 ± 0.16 (1.52%)
	P value		1.00	1.00	1.00	1.00
T_2^* bicomponent	T_{2S}^* (ms)	0.29 ± 0.03	0.29 ± 0.02 (−1.30%)	0.28 ± 0.02 (−2.81%)	0.28 ± 0.02 (−4.61%)	0.27 ± 0.02 (−6.11%)
	P value		0.96	0.73	0.23	0.05
	T_{2L}^* (ms)	7.24 ± 1.76	7.30 ± 1.70 (0.75%)	7.36 ± 1.65 (1.59%)	7.35 ± 1.60 (1.47%)	7.31 ± 1.62 (0.89%)
	P value		1.00	0.99	0.99	1.00
	Fraction short (%)	75.2 ± 4.4	73.9 ± 4.8 (−1.70%)	73.7 ± 4.9 (−2.00%)	73.2 ± 5.2 (−2.68%)	72.5 ± 5.5 (−3.51%)
	P value		0.87	0.79	0.58	0.35
T_1 (ms)		222.7 ± 26.4	223.9 ± 27.1 (0.58%)	224.0 ± 28.4 (0.62%)	224.6 ± 28.1 (0.89%)	224.6 ± 28.4 (0.84%)
	P value		1.00	1.00	0.99	0.99
MTR (%) (1500°, 2 kHz)		0.37 ± 0.06	0.36 ± 0.06 (−3.63%)	0.36 ± 0.06 (−3.72%)	0.35 ± 0.06 (−4.14%)	0.35 ± 0.06 (−4.31%)
	P value		0.93	0.92	0.88	0.87
Macromolecular fraction (%)		56.6 ± 12.4	56.3 ± 11.6 (−0.46%)	56.0 ± 13.8 (−1.13%)	56.2 ± 13.2 (−0.68%)	56.5 ± 11.9 (−0.25%)
	P value		0.99	1.00	1.00	1.00
Sampling window (μs)		688	992	1200	1392	1600
Acceleration factor		1	2.6	3.5	4.1	5.0

Note: Errors (%) and *P* values from Dunnett's test compare the results of each UTE Cones trajectory with PR results.
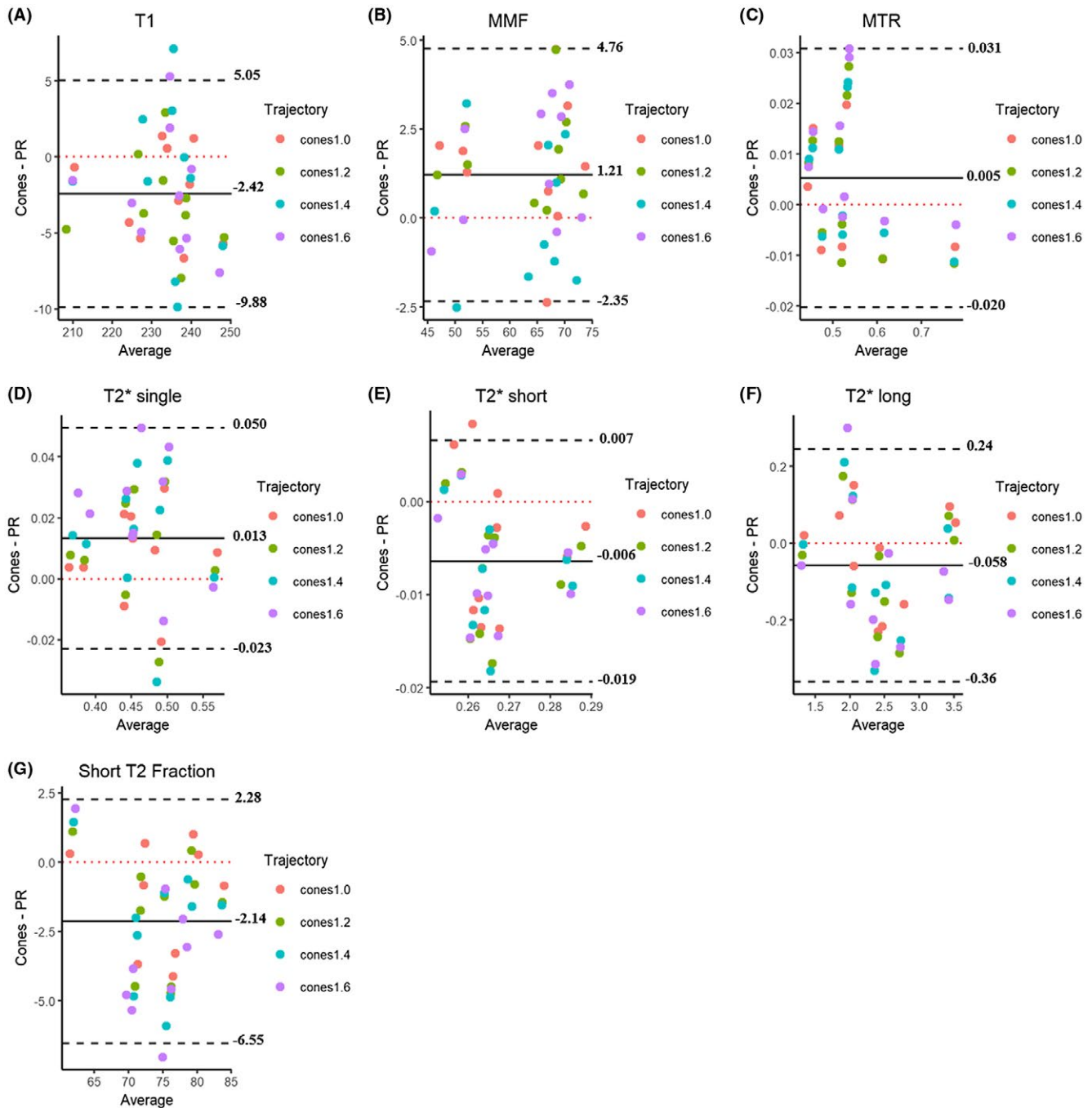
FIGURE 5 Bland-Altman plots of biomarkers T_1 (A), macromolecular fraction (MMF) (B), Magnetization transfer ratio (MTR) (C), T_2^* (D), short T_2^* (E), long T_2^* (F), and short T_2^* fraction (G) for bovine cortical bone samples comparing various Cones sampling trajectories with radial trajectory. The 2 dashed black lines indicate the 95% upper and lower limits of agreement, respectively, and the black line indicates the level of average difference

reduce the total scan time while retaining the measurement accuracy within an acceptable range. The results are likely to help in developing translational quantitative 3D Cones UTE imaging of cortical bone and other musculoskeletal tissues.

The 3D spiral trajectories require no phase encoding at the beginning of readout and begin at the center of k-space, making them suitable for UTE acquisitions. The spiral trajectory has significantly higher efficiency in filling k-space than the radial trajectory.[35] Stretching the spiral trajectory results in a further increased readout time (sampling window length) and a much decreased number of readouts, because outer k-space is more efficiently sampled. This leads to a much shorter scan time as well as a more uniform sampling density, which improves SNR efficiency.[36] Potential disadvantages of the increased readout time are increased flow effects and off-resonance blurring, as well as greater sensitivity to T_2^* decay.[36]
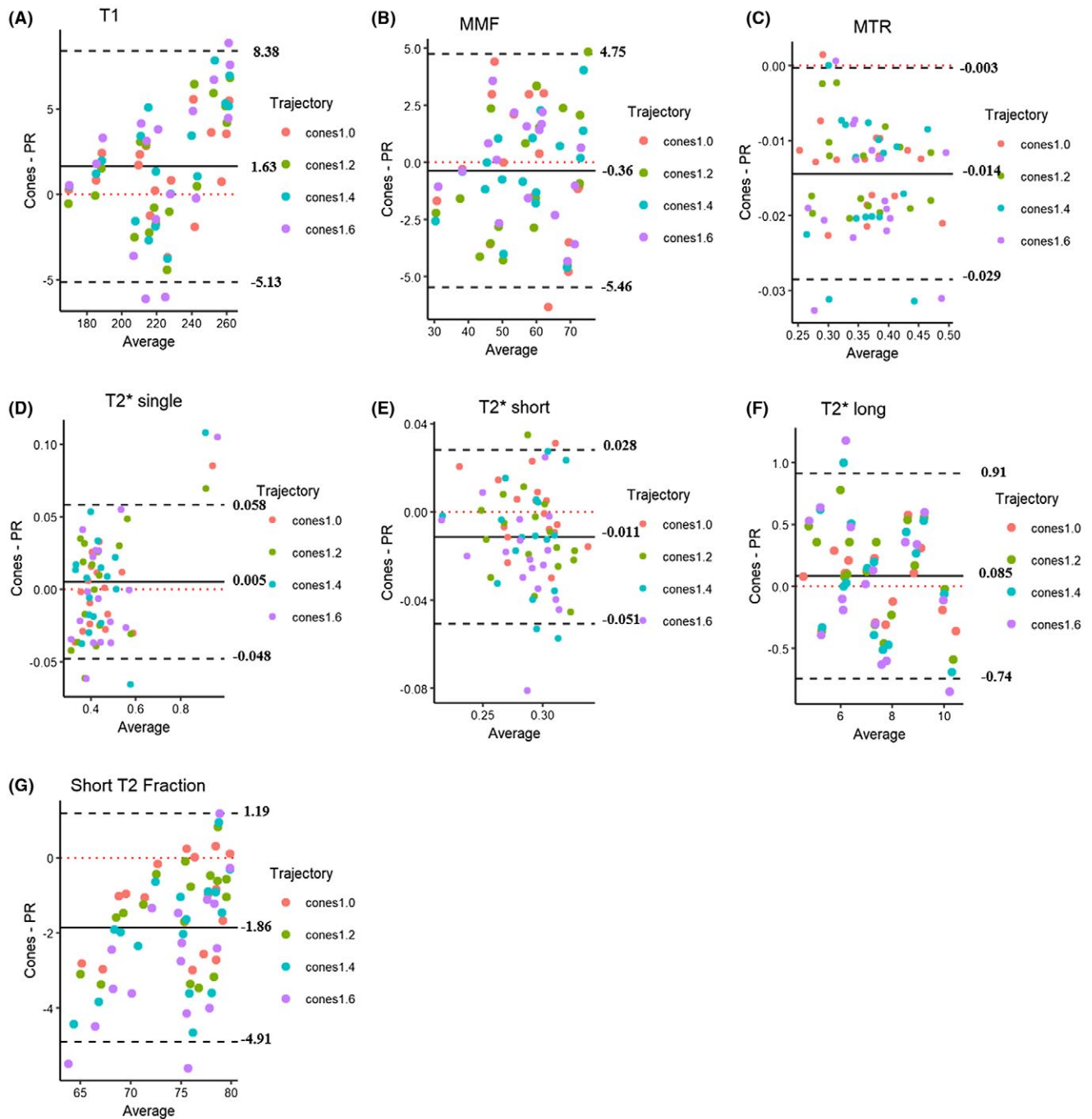
FIGURE 6 Bland-Altman plots of biomarkers T_1 (A), macromolecular fraction (MMF) (B), MTR (C), T_2^* (D), short T_2^* (E), long T_2^* (F) and short T_2^* fraction (G) for human cortical bone samples comparing various Cones sampling trajectories with radial trajectory. The 2 dashed black lines indicate the 95% upper and lower limits of agreement, respectively, and the black line indicates the level of average difference

Few studies have focused on the optimization of the sampling window length. Rahmer et al[26] investigated an optimal acquisition time for 3D radial UTE imaging, and 0.81 times the T_2 value was suggested for maximal SNR. However, Rahmer's study did not consider the effect of ramp sampling, which might play a major role in optimizing SNR and spatial resolution. Furthermore, the spatial resolution might be rather low and suboptimal for many musculoskeletal imaging applications when such a short sampling window is used.

Du et al[27] investigated the effect of different spiral sampling durations on short T_2 spatial blurring in 2D UTE imaging and demonstrated that increased sampling window resulted in more blurring (or spatial resolution reduction), but higher SNR. A spiral sampling window of 2 to 4 times the T_2^* value was suggested for in vivo imaging of short T_2 tissues to obtain a balance between spatial resolution and SNR.

The current study is the first study to investigate the effects of sampling window length on UTE-based quantitative

biomarkers, using ex vivo analysis of bovine and human cortical bone samples. No significant differences were observed for the calculated UTE biomarkers (T_1, macromolecular fraction and MTR, single-component T_2^*, bicomponent T_2^*) between the radial sampling trajectory (688 μs) and spiral sampling trajectories with a duration of 992 μs to 1600 μs. One possible explanation would be that quantitative imaging of a low spatial frequency object relies more on central k-space and may be less sensitive to short T_2 blurring than morphological imaging.

The results of this study indicate that quantitative UTE MRI of low spatial frequency objects can be greatly accelerated with longer spiral sampling windows (i.e., 992 μs to 1600 μs) without substantial measurement errors (Tables 1 and 2). Errors were all within 3% in T_1, macromolecular fraction, and MTR for bovine bone samples, whereas errors were within 5% for human bone samples when the sampling window was 1600 μs or shorter. Errors in T_2^* biomarkers were all within 5% when the sampling window was 1392 μs or shorter for both bovine and human bone specimens. Thus, a recommended sampling window time could be about 1392 μs, which can decrease the total scan time by 76% with respect to radial sampling. Furthermore, the UTE biomarkers obtained in the current study were largely consistent with the values reported in previous studies.[16,37,38]

Both single-component and bicomponent T_2^* analyses were more sensitive to the effect of extended sampling windows compared with T_1, macromolecular fraction, and MTR. There are multiple factors contributing to the increased errors, including the high sensitivity of T_2^* to B_0 field inhomogeneity and local susceptibility, as well as the very different response of short and long T_2^* components to extended sampling windows.[39] Thus, the robustness of T_1 and MT modeling analysis is slightly higher than T_2^* analysis. Eddy currents may affect the quantification accuracy for all UTE biomarkers, as radial and spiral samplings are sensitive to eddy current–related gradient distortions.

There are several limitations in our study. First, the choice of spiral sampling windows was arbitrary, with 4 windows chosen to compare a wide range of sampling window lengths. More sampling windows could be tested within the range of 992 μs and 1600 μs to further optimize the scan time. Increased artifacts were observed when the sampling window was longer than 1600 μs, likely due to increased eddy currents and off-resonance effects. Second, we imaged cortical bone of the tibial midshaft, which has a cylindrical shape with primarily low-frequency components that do not require high spatial resolution for morphological imaging, and placed ROIs on the outer two-thirds band to minimize influences from fat. Therefore, the results have only been shown to hold for low spatial frequency objects. Third, this study was done ex vivo, with soft tissues surrounding the bone removed, a situation that may differ from the physiological situation. We removed the surrounding tissues to avoid the chemical shift artifacts of fat so that it is clear that the assessed artifacts are from the stretching sampling windows. Our results suggest that 3D UTE-Cones with an extended sampling window can be used to quantitatively image thick segments of cortical bone without significant errors and with a greatly reduced scan time. Extending these results to thinner cortical bone or cortical bone near the endosteum—which may be contaminated by chemical shift artifacts from bone marrow fat—will require further studies using advanced fat-suppression methods with minimal effect on water excitation as well as confirmation of these results with intact *ex vivo* joints and *in vivo* human studies. Fourth, this study was focused only on cortical bone. The effects of the extended sampling window on other musculoskeletal tissues, such as articular cartilage, menisci, tendons and ligaments, should be investigated; however, these tissues have longer T_2 values than cortical bone and should experience less T_2^* decay during longer sampling windows. Finally, the radial trajectory was used as the reference standard, but it is also subject to measurement error and bias.

5 | CONCLUSIONS

Compared with radial sampling, quantitative UTE-MRI techniques using spiral trajectories with extended sampling windows were able to reduce scan time without major effects on quantification accuracy of T_1, single-component T_2^*, bicomponent short and long T_2^* and relative fractions, MTR, and macromolecular fraction in low spatial frequency objects, such as cortical bone of the tibial midshaft. Our recommended sampling window for human cortical bone was about 1392 μs, resulting in an acceleration factor of 4.1 and measurement errors typically less than 5% in all UTE biomarkers.

This study suggests that quantitative UTE-MRI techniques can be greatly accelerated with longer sampling windows without significant quantification errors in low spatial frequency objects such as midshaft tibia. These results are expected to facilitate clinical imaging of cortical bone using accelerated quantitative 3D UTE-Cones techniques.

ORCID

Lidi Wan https://orcid.org/0000-0001-6851-4583

REFERENCES

1. Du J, Bydder GM. Qualitative and quantitative ultrashort-TE MRI of cortical bone. *NMR Biomed*. 2013;26:489–506.

2. Bell KL, Loveridge N, Jordan GR, Power J, Constant CR, Reeve J. A novel mechanism for induction of increased cortical porosity in cases of intracapsular hip fracture. *Bone*. 2000;27:297–304.

3. Stein EM, Silva BC, Boutroy S, et al. Primary hyperparathyroidism is associated with abnormal cortical and trabecular microstructure and reduced bone stiffness in postmenopausal women. *JAMA*. 2013;28:1029–1040.

4. Burghardt AJ, Issever AS, Schwartz AV, et al. High-resolution peripheral quantitative computed tomographic imaging of cortical and trabecular bone microarchitecture in patients with type 2 diabetes mellitus. *J Clin Endocrinol Metab*. 2010;95:5045–5055.

5. Newman CL, Moe SM, Chen NX, et al. Cortical bone mechanical properties are altered in an animal model of progressive chronic kidney disease. *PLoS ONE*. 2014;9:e99262.

6. Schaffler MB, Burr DB. Stiffness of compact bone: effects of porosity and density. *J Biomech*. 1988;21:13–16.

7. Diab T, Vashishth D. Effects of damage morphology on cortical bone fragility. *Bone*. 2005;37:96–102.

8. Wehrli FW, Song HK, Saha PK, Wright AC. Quantitative MRI for the assessment of bone structure and function. *NMR Biomed*. 2006;19:731–764.

9. Horch RA, Nyman JS, Gochberg DF, Dortch RD, Does MD. Characterization of 1H NMR signal in human cortical bone for magnetic resonance imaging. *Magn Reson Med*. 2010;64:680–687.

10. Robson MD, Gatehouse PD, Bydder M, Bydder GM. Magnetic resonance: an introduction to ultrashort TE (UTE) imaging. *J Comput Assist Tomogr*. 2003;27:825–846.

11. Du J, Bydder M, Takahashi AM, Carl M, Chung CB, Bydder GM. Short T2 contrast with three-dimensional ultrashort echo time imaging. *Magn Reson Imaging*. 2011;29:470–482.

12. Du J, Takahashi AM, Bydder M, Chung CB, Bydder GM. Ultrashort TE imaging with off-resonance saturation contrast (UTE-OSC). *Magn Reson Med*. 2009;62:527–531.

13. Du J, Takahashi AM, Bae WC, Chung CB, Bydder GM. Dual inversion recovery, ultrashort echo time (DIR UTE) imaging: creating high contrast for short-T(2) species. *Magn Reson Med*. 2010;63:447–455.

14. Du J, Carl M, Bydder M, Takahashi A, Chung CB, Bydder GM. Qualitative and quantitative ultrashort echo time (UTE) imaging of cortical bone. *J Magn Reson*. 2010;207:304–311.

15. Ma YJ, Chang EY, Bydder GM, Du J. Can ultrashort-TE (UTE) MRI sequences on a 3-T clinical scanner detect signal directly from collagen protons: freeze-dry and D2 O exchange studies of cortical bone and Achilles tendon specimens. *NMR Biomed*. 2016;29:912–917.

16. Ma YJ, Tadros A, Du J, Chang EY. Quantitative two-dimensional ultrashort echo time magnetization transfer (2D UTE-MT) imaging of cortical bone. *Magn Reson Med*. 2018;79:1941–1949.

17. Reichert IL, Robson MD, Gatehouse PD, et al. Magnetic resonance imaging of cortical bone with ultrashort TE pulse sequences. *Magn Reson Imaging*. 2005;23:611–618.

18. Techawiboonwong A, Song HK, Leonard MB, Wehrli FW. Cortical bone water: in vivo quantification with ultrashort echo-time MR imaging. *Radiology*. 2008;248:824–833.

19. Bae WC, Chen PC, Chung CB, Masuda K, D'Lima D, Du J. Quantitative ultrashort echo time (UTE) MRI of human cortical bone: correlation with porosity and biomechanical properties. *JBMR*. 2012;27:848–857.

20. Marcon M, Weiger M, Keller D, et al. Magnetization transfer imaging of cortical bone in vivo using a zero echo time sequence in mice at 4.7 T: a feasibility study. *MAGMA*. 2016;29:853–862.

21. Ma YJ, Chang EY, Carl M, Du J. Quantitative magnetization transfer ultrashort echo time imaging using a time-efficient 3D multispoke Cones sequence. *Magn Reson Med*. 2018;79:692–700.

22. Nyman JS, Ni Q, Nicolella DP, Wang X. Measurements of mobile and bound water by nuclear magnetic resonance correlate with mechanical properties of bone. *Bone*. 2008;42:193–199.

23. Horch RA, Gochberg DF, Nyman JS, Does MD. Non-invasive predictors of human cortical bone mechanical properties: T(2)-discriminated H NMR compared with high resolution X-ray. *PLoS ONE*. 2011;6:e16359.

24. Chang EY, Bae WC, Shao H, et al. Ultrashort echo time magnetization transfer (UTE-MT) imaging of cortical bone. *NMR Biomed*. 2015;28:873–880.

25. Jerban S, Ma YJ, Nazaran A, et al. Detecting stress injury (fatigue fracture) in fibular cortical bone using quantitative ultrashort echo time-magnetization transfer (UTE-MT): an ex vivo study. *NMR Biomed*. 2018;31:e3994.

26. Rahmer J, Bornert P, Groen J, Bos C. Three-dimensional radial ultrashort echo-time imaging with T2 adapted sampling. *Magn Reson Med*. 2006;55:1075–1082.

27. Du J, Bydder M, Takahashi AM, Chung CB. Two-dimensional ultrashort echo time imaging using a spiral trajectory. *Magn Reson Imaging*. 2008;26:304–312.

28. King KF, Foo TK, Crawford CR. Optimized gradient waveforms for spiral scanning. *Magn Reson Med*. 1995;34:156–160.

29. Jackson JI, Nishimura DG, Macovski A. Twisting radial lines with application to robust magnetic resonance imaging of irregular flow. *Magn Reson Med*. 1992;25:128–139.

30. Chen J, Carl M, Ma Y, et al. Fast volumetric imaging of bound and pore water in cortical bone using three-dimensional ultrashort-TE (UTE) and inversion recovery UTE sequences. *NMR Biomed*. 2016;29:1373–1380.

31. Ma YJ, Lu X, Carl M, et al. Accurate T1 mapping of short T2 tissues using a three-dimensional ultrashort echo time cones actual flip angle imaging-variable repetition time (3D UTE-Cones AFI-VTR) method. *Magn Reson Med*. 2018;80:598–608.

32. Yarnykh VL. Actual flip-angle imaging in the pulsed steady state: a method for rapid three-dimensional mapping of the transmitted radiofrequency field. *Magn Reson Med*. 2007;57:192–200.

33. Takahashi A, Peters T. Compensation of multi-dimensional selective excitation pulses using measured k-space trajectories. *Magn Reson Med*. 1995;34:446–456.

34. Springer F, Martirosian P, Machann J, Schwenzer NF, Claussen CD, Schick F. Magnetization transfer contrast imaging in bovine and human cortical bone applying an ultrashort echo time sequence at 3 Tesla. *Magn Reson Med*. 2009;61:1040–1048.

35. Addy NO, Ingle RR, Wu HH, Hu BS, Nishimura DG. High-resolution variable-density 3D cones coronary MRA. *Magn Reson Med*. 2015;74:614–621.

36. Gurney PT, Hargreaves BA, Nishimura DG. Design and analysis of a practical 3D cones trajectory. *Magn Reson Med*. 2006;55:575–582.

37. Biswas R, Bae W, Diaz E, et al. Ultrashort echo time (UTE) imaging with bi-component analysis: bound and free water

evaluation of bovine cortical bone subject to sequential drying. *Bone*. 2012;50:749–755.

38. Chen J, Grogan SP, Shao H, et al. Evaluation of bound and pore water in cortical bone using ultrashort-TE MRI. *NMR Biomed*. 2015;28:1754–1762.

39. Du J, Diaz E, Carl M, Bae W, Chung CB, Bydder GM. Ultrashort echo time imaging with bicomponent analysis. *Magn Reson Med*. 2012;67:645–649.

How to cite this article: Wan L, Zhao W, Ma Y, et al. Fast quantitative 3D ultrashort echo time MRI of cortical bone using extended cones sampling. *Magn Reson Med*. 2019;00:1–12. https://doi.org/10.1002/mrm.27715